

SPECTRAL CLASSES AND SURFACE PROPERTIES OF THE SATURNIAN SATELLITES RETRIEVED FROM CASSINI-VIMS DISK-INTEGRATED OBSERVATIONS.

G. Filacchione¹, F. Capaccioni¹, R. N. Clark², D. P. Cruikshank³, A. Coradini⁴, P. Cerroni¹, M. Ciarniello¹, F. Tosi⁴, P. D. Nicholson⁵, T. B. McCord⁶, R. H. Brown⁷, B. J. Buratti⁸, R. M. Nelson⁸, R. Jaumann⁹, K. Stephan⁹. ¹INAF-IASF, via del Fosso del Cavaliere, 100, Rome, Italy; ²U.S. Geological Survey, Denver, CO, USA; ³NASA Ames Research Center, Moffett Field, CA, USA; ⁴INAF-IFSI, via del Fosso del Cavaliere, 100, Rome, Italy; ⁵Cornell University, Astronomy Department, Ithaca, NY, USA; ⁶Bear Fight Center, Winthrop, WA, USA; ⁷Lunar and Planetary Lab and Steward Observatory, University of Arizona, Tucson, AZ, USA; ⁸Jet Propulsion Laboratory, California Institute of Technology, Pasadena, CA, USA; ⁹Institute for Planetary Exploration, DLR, Berlin, Germany.

Introduction: We present an update of the analysis of the Saturnian satellites disk-integrated observations returned by the VIMS experiment (Visual and Infrared Mapping Spectrometer) on board Cassini. This investigation is focused on the study of the VIS spectral slopes and IR absorption bands variability. Both these parameters can be used as indicators of the compositions and properties of the satellite surfaces.

Observations: thanks to VIMS, a comprehensive hyperspectral view of the icy moons orbiting in the saturnian system is available, allowing us to perform a comparative analysis of their properties. After having analyzed the data returned during the Cassini's nominal mission [1, 2], we are continuing to process more recent disk-integrated observations. In this work we are using about 2000 observations (spanning from June 2004 to March 2009), a statistically significant dataset that includes the principal satellites Mimas, Enceladus, Tethys, Dione, Rhea, Hyperion, Iapetus as well as the minor moons Atlas, Prometheus, Pandora, Janus, Epimetheus, Telesto, Calypso and Phoebe.

VIS-IR disk integrated reflectance spectra: I/F spectra of Saturn's satellites (see Fig. 1) are characterized by a step red slope in the 0.35-0.55 μm range, which is highly diagnostic of the presence of organic contaminants and darkening agents mixed to ice particles; in the 0.55-0.95 μm range the spectra are generally more flat and featureless [1, 2]. In the IR range the water ice bands at 1.5-2.0-3.0 μm bands are evident everywhere, while the CO₂ ice band at 4.26 μm is seen only on the three external satellites Hyperion, Iapetus and Phoebe [3, 4]. Some spectral features that are evident in spectra having high spatial resolution are very difficult to recognize in disk-integrated spectra [5]. Despite these limitations, VIMS dataset can be used to derive some specific spectrophotometric indicators for the study of the macroscopic properties of the surfaces' ices. In the next two paragraphs we'll focus on the correlations among the 0.35-0.55 μm spectral slope vs. 2.0 μm band depth and on the 1.25 vs. 1.5 μm water ice band depths. The first is an indicator of the amount of contaminants mixed on the surfaces while the second is sensitive to both regolith grain size and composition.

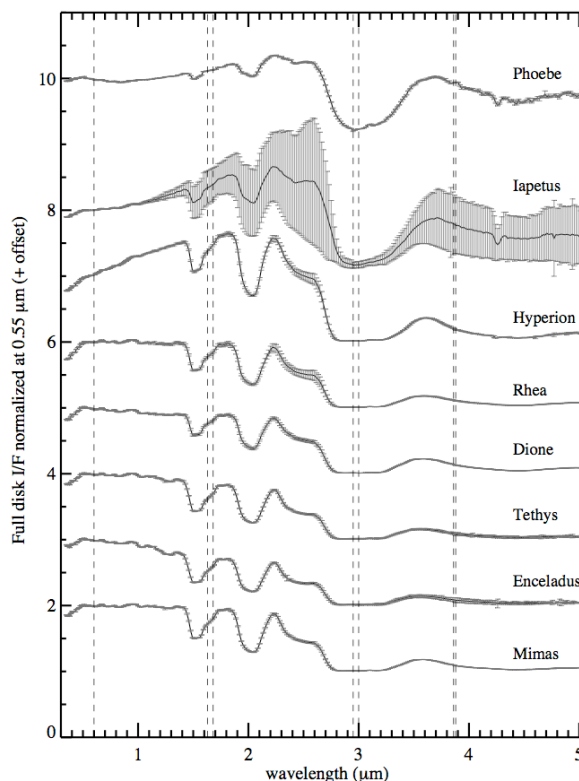


Figure 1: Average disk-integrated I/F spectra of the principal satellites of Saturn and Phoebe measured by Cassini-VIMS. Vertical lines correspond to instrumental order sorting filter gaps. Each spectrum is normalized at 0.55 μm and stacked with an offset for better visualization. For each channel the variability of the spectrum at 1 standard deviation is indicated.

VIS spectral slope vs. IR water ice band depth. The amount of contaminants mixed with ice on the saturnian satellites can be retrieved by a simultaneous analysis of VIS slope in the the 0.35-0.55 μm interval and IR water ice band depth at 2.0 μm [2]. The resulting scatterplot for these two indicators is shown in Fig. 2, from which it is evident that the Saturn's satellites are grouped in four distinct classes: 1) Enceladus, Tethys and Mimas have the strongest 2.0 μm band depth and a small (thus bluer) 0.35-0.55 μm visible slope. Their bluer surfaces are therefore made by almost pure water ice mixed with small percentage of

contaminants; 2) Rhea observations have an intermediate $2.0\ \mu\text{m}$ band depth but the highest visible slope of the group (up to $2.2\ \mu\text{m}^{-1}$). The contaminants therefore must influence mainly the VIS range; 3) Organics- and carbon dioxide-rich Iapetus and Phoebe are clustered in the lower-left corner of the scatterplot, having both small $2.0\ \mu\text{m}$ band depth and $0.35\text{-}0.55\ \mu\text{m}$ visible slope. These satellites have the largest amount of contaminants among the icy satellites of Saturn. Some small clusters of Iapetus trailing hemisphere observations are grouped towards higher slopes and band depths; 4) Hyperion and Dione are intermediate among the previous three classes having a $2.0\ \mu\text{m}$ BD between $0.2\text{-}0.4$ and VIS slope between $1.0\text{-}1.7\ \mu\text{m}^{-1}$.

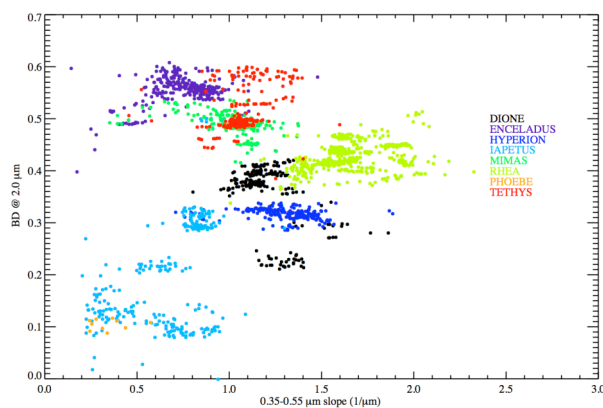


Figure 2: Scatterplot of the $0.35\text{-}0.55\ \mu\text{m}$ visible spectral slope vs. the $2.0\ \mu\text{m}$ water ice band depth (BD) for the principal satellites of Saturn. Each point corresponds to a disk integrated observation.

Water ice band depths and regolith grain sizes. An indication of the regolith particle sizes on the satellite surfaces can be obtained by means of a comparison of the observed water ice band depths with laboratory measurements [5]. To perform this test we use the $1.25\ \mu\text{m}$ vs. $1.5\ \mu\text{m}$ band depth (BD) scatterplot (Fig. 3) in which we compare the distribution of the satellites points with respect to reference values measured in lab on water ice grain particles of very different sizes (from $1\ \mu\text{m}$ up to $100\ \mu\text{m}$). The satellites' band depths are clustered along a diagonal branch that includes the more icy objects (Enceladus, Tethys, Calypso, Telesto) on the top end, or at the strongest band depths, then satellites with intermediate contamination in the middle (Rhea, Mimas, Dione, Janus) and finally the organic-rich Iapetus, Hyperion and Phoebe, which have the faintest band depths of the group. This distribution, despite biased by the contaminants, can be compared with the BD values measured on pure water ice grains (indicated by blue crosses in Fig. 3). At least for the more icy satellites at the top end we can assume that the band depth is weakly influenced by contaminants

and therefore can be used as a good indicator for the water ice grain sizes. From comparison with lab measurements we observe that the surfaces of Enceladus, Tethys, Calypso and Telesto should be made up of grains of about $50\ \mu\text{m}$. For the remaining satellites it is more difficult to determine the grain sizes because the values are biased by the increasing amount of contaminants, which change the surfaces' composition. Finally some Enceladus observations at high phase angle ($130^\circ\text{-}140^\circ$ indicated in Fig. 3) have an anomalous increase in the $1.25\ \mu\text{m}$ band depth: this effect could be real and correlated with the plume activity, or could be an instrumental artifact introduced by a hot pixel in the detector at $\lambda=1.22\ \mu\text{m}$.

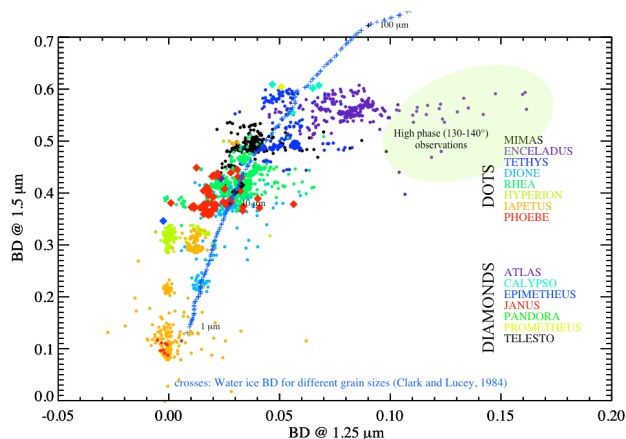


Figure 3: Scatterplot of the $1.25\ \mu\text{m}$ vs. $1.5\ \mu\text{m}$ water ice band depths (BD) for the principal (dots) and minor satellites (diamonds) of Saturn. Crosses indicate the band depth values for grains ranging from 1 to $100\ \mu\text{m}$ (lab measurements by Clark and Lucey, 1984).

Conclusions. This comparative method when applied to the VIMS dataset is able to classify the spectral characteristics of the saturnian system satellites, as well as to trace the radial variability of the properties of water ice and contaminants across the system. Such results could help us decipher the origins and evolutionary history of the satellites orbiting in Saturn's system.

References: [1] Filacchione, G. et al, (2007) *Icarus*, 186, 259-290. [2] Filacchione, G. et al, (2010) *Icarus*, in press. [3] Cruikshank, D. P., et al. (2007) *Nature*, 448, 54-56. [4] Cruikshank, D. P., et al. (2008) *Icarus*, 193, 334-343. [5] Clark, R. N. et al. (2008) *Icarus*, 193, 372-386.